

# Kolmogorov-Smirnov test as a tool to study the distribution of ultra-high energy cosmic ray sources

D. Harari, S. Mollerach and E. Roulet  
CONICET, Centro Atómico Bariloche,  
Av. Bustillo 9500, Bariloche, 8400, Argentina

February 11, 2022

## Abstract

We analyze in detail the two-dimensional Kolmogorov-Smirnov test as a tool to learn about the distribution of the sources of the ultra-high energy cosmic rays. We confront in particular models based on AGN observed in X rays, on galaxies observed in HI and isotropic distributions, discussing how this method can be used not only to reject isotropy but also to support or reject specific source models, extending results obtained recently in the literature.

## 1 Introduction

One of the most puzzling aspects of cosmic rays (CRs) is the enormous energies they can reach, which can be up to seven orders of magnitude higher than those being achieved in the most powerful human-made accelerator. The astrophysical sites where the acceleration of these particles takes place have then to be quite extreme, and their identification is of paramount importance to understand the CR origin and the mechanisms capable of producing them.

For observed energies larger than  $E_{GZK} = 6 \times 10^{19}$  eV, CRs cannot come from very far away because if they were produced e.g. from beyond  $\sim 200$  Mpc, no matter what was the initial value of their energy at the source it would likely be degraded below  $E_{GZK}$  by the time they reach us, due to the interactions with the cosmic microwave background that take place during the CR propagation [1]. A suppression of the CR flux at the highest energies compatible with this phenomenon has indeed been measured recently [2, 3]. This suggests that above  $E_{GZK}$  only nearby sources contribute to the observed CR fluxes. Moreover, since at these high energies the CR trajectories are not expected to suffer very large deflections in the galactic or extragalactic magnetic fields (at least if the CR charges are not too large), it is to be expected that the inhomogeneous distribution of the potential sources in our cosmic neighborhood will give rise to an anisotropic pattern of CR arrival directions.

The search for the sources of the ultra-high energy (UHE) CRs got renewed interest after data from the Pierre Auger Observatory revealed a correlation between the arrival directions of the highest energy events (with  $E > 57$  EeV, where  $1 \text{ EeV} \equiv 10^{18}$  eV) and the directions towards the active galactic nuclei (AGN) closer than about 100 Mpc [4]. The maximum significance for this correlation was obtained for angular separations between events and AGN smaller than  $3.2^\circ$  and for AGN closer than 71 Mpc, for which 20 events out of 27 were found to correlate while only 5.6 correlations were expected to arise by chance from an isotropic distribution. This indeed suggests that the angular deflections are not too large at the highest energies (although of course the closest AGN to an event need not necessarily be its source) and gives further support to the idea that the spectral suppression is due to the GZK effect, not just to the exhaustion of the acceleration power of the sources. The correlation found in data from the Auger Observatory by no means proves that the AGN are the actual sources of the CRs, because these active galaxies could well be acting

as tracers of the nearby large scale structure which also hosts other types of galaxies or possible acceleration sites (such as gamma ray bursts). Even if AGN are the sources, it may well be that only a particular subclass of the vast compilation contained in the Véron-Cetty and Véron catalog (VC catalog) used to establish the correlation, or even some obscured AGN absent in the catalog, are the actual sources of the highest energy CRs. Hence, further analyses can be important to shed some light on this issue.

There have been in particular two recent analyses trying to find indications about the possible UHECR source population using the two dimensional Kolmogorov-Smirnov (2DKS) test. The first by George et al. [5] confronted the arrival directions of the Auger events above 57 EeV with the positions of the X ray selected AGN in the SWIFT BAT catalog [6], updated with the first 22 months of data. The second, by Ghisellini et al. [7], confronted those same events with the HIPASS catalog of HI selected radio galaxies from the All-Sky Parkes Survey [8, 9]. The first analysis concluded that although the standard 2DKS didn't give much hints of correlations, restricting the AGN to those closer than 100 Mpc and weighting them by their X ray luminosities led to a correlation of  $\sim 98\%$ , giving hence additional support to the Auger Observatory results. The second analysis, weighting the HIPASS galaxies by their HI flux found a correlation of only  $\sim 72\%$ , which increased to 99% after restricting the test to the southern equatorial sample (which is more complete) and to the more massive galaxies (with HI mass greater than  $1.1 \times 10^{10} M_{\odot}$ ). In this work we want to reconsider this kind of analyses and discuss further issues which can help to understand what is being tested with the 2DKS method, hoping that this will be useful for future studies of this type.

## 2 The 2DKS test

In one dimension  $X$ , the Kolmogorov-Smirnov test looks for the maximum value  $D$  of the difference between the fractional cumulative distribution of the variable  $X$  measured in the data and that expected for a model. The significance of that departure can be obtained analytically from the expected distribution of  $D$  in the case of the null-hypothesis (data drawn from the model) or alternatively estimated from the fraction of samples simulated according to the model which give rise to larger departures  $D$  than the data themselves. Note that the maximum departure will always be found at one of the values of  $X$  realized by the data, as can be easily understood from the step-like behavior of the cumulative distribution. Also note that by looking to the cumulative distribution at one of the data points  $X_i$ , the one-dimensional KS test compares the fraction of data points with  $X < X_i$  with the corresponding fraction expected in the model.

The generalization of this method for two dimensions,  $X$  and  $Y$ , consists of looking for the fractions in each of the four natural quadrants (adopting a specific set of coordinates, typically the equatorial ones for astronomical applications) of both the data and a model, which may correspond e.g. to directions drawn from the locations of the objects contained in a given catalog. Then one finds the reference point and the quadrant for which the difference between the two fractions is maximal. In the original proposal of Peacock [10], the reference points are all the possible combinations  $X_i, Y_j$ , where  $i$  and  $j$  refer to any of the data points. In the modified test proposed by Fasano and Franceschini [11], which is much less demanding computationally and has similar power, one just chooses as reference points the locations of the different data points  $X_i, Y_i$ . Alternatively, in the so-called two-sample test one first finds the distance  $D_1$  obtained using all data points as reference, then the distance  $D_2$  obtained using instead the coordinates of the objects in the catalog as reference points, and finally considers their average  $\bar{D} \equiv (D_1 + D_2)/2$  as a measure of the distance between the two distributions. For large data (and catalog) sets the two approaches should give similar results. For definiteness we will consider hereafter the distances obtained in the two-sample case.

What the 2DKS test ultimately probes is whether the data are distributed in the sky in the same proportion as the model, and achieves that by checking if there is any quadrant in which the fraction of the data points is significantly different from the corresponding fraction of the catalog

objects present. In particular, large deviations are expected if the data points are unrelated to the model considered, but also if they correspond to a subsample of the objects in the model having a different overall distribution. Similarly, if only a subset of the catalog objects considered are the actual sources, the extra ones may ruin the agreement in the comparison, and only after appropriate cuts the source population may be identified using this method. On the other hand, if the actual sources are different from those in the model but have anyway a similar spatial distribution (e.g. one being a tracer of the other) the 2DKS test will indicate a good agreement even if the model does not correspond to the true sources. George et al.[5] generalized this method by considering the fractions obtained after weighting each object in the catalog by the relative exposure of the Observatory in the corresponding region of the sky and also weighting it by its flux. Since ref. [5] considered as potential sources the AGN identified by SWIFT, they were weighted by the flux measured in X rays, as could be expected if the CR luminosities were proportional to the X ray ones. Similarly ref. [7] obtained the fractions for the HIPASS based model weighting the galaxies by their integrated HI fluxes as well as the exposure of the Auger Observatory.

A probability of correlation was then quoted as a measure of the significance of the results. It is defined as the fraction of isotropic simulated sets of arrival directions giving departures  $D$  larger than those found in the actual data, comparing both the real and simulated sets to the same source model, i.e. to the same reference catalog. Note that this gives a measure of the discrepancy between the data and the isotropic simulations rather than a direct measure of the agreement between the data and the model, i.e. it tells how worse the isotropic simulations do under a similar test rather than how typical of a model realization the data are. One of the purposes of the present paper is to introduce both ingredients into the application of the 2DKS test to the search for a satisfactory UHECR source model. To stress the point that the correlation probability gives just a measure of the departure from isotropy we will hereafter refer to it instead by the name of ‘anisotropy probability’.

Let us finally note that if the data are a fair realization of the model being tested, the distances  $D$  obtained will just be the result of statistical fluctuations due to the limited sampling, and are hence expected to decrease with the size of the data sample  $n$  as  $n^{-1/2}$ . It is then customary to use as an alternative to  $D$  the quantity  $Z = D\sqrt{n}$ , which would remain approximately constant with increasing  $n$ . However, if the data are not a fair sample of the model there will be a typical distance between the true distribution sampled by the data and the model being considered. This means that there will be one particular quadrant with respect to one particular sky direction for which the difference in the fractions of the true distribution and the model distribution is maximal, and this difference  $D$  will have a certain fixed value to which the data will ultimately approach with very large statistics. Hence, in this case the quantity  $Z$  is expected to grow with the size of the data sample.

When the two-sample case mentioned previously is considered, an effective value  $n_{eff} \equiv n_1 n_2 / (n_1 + n_2)$  is adopted in the definition  $Z = \overline{D}\sqrt{n_{eff}}$ , with  $n_1$  the number of data points and  $n_2$  the number of catalog points [10]. Anyway, since the significance is obtained by comparing the data with the results of isotropic simulations with the same number of events, it doesn’t matter whether  $\overline{D}$  or  $Z$  are compared. We will hence display the results for  $\overline{D}$  (omitting hereafter the overline) because the interpretation in terms of the difference in fractions has a more direct meaning than the quantity  $Z$ . We note that when comparing the expected distances for a model compared against itself, an analytic expression for the probability to obtain a certain value can be derived [11, 12], but in the general case in which the model is different that the reference catalog the use of simulations is required.

### 3 Results

Fig. 1 shows the resulting distances taking as reference objects the AGN in the 22 months SWIFT BAT catalog [13] with different cuts and weights. This catalog contains 163 AGN identified in X rays with reliably measured flux and redshift and within the field of view of the Auger Observatory

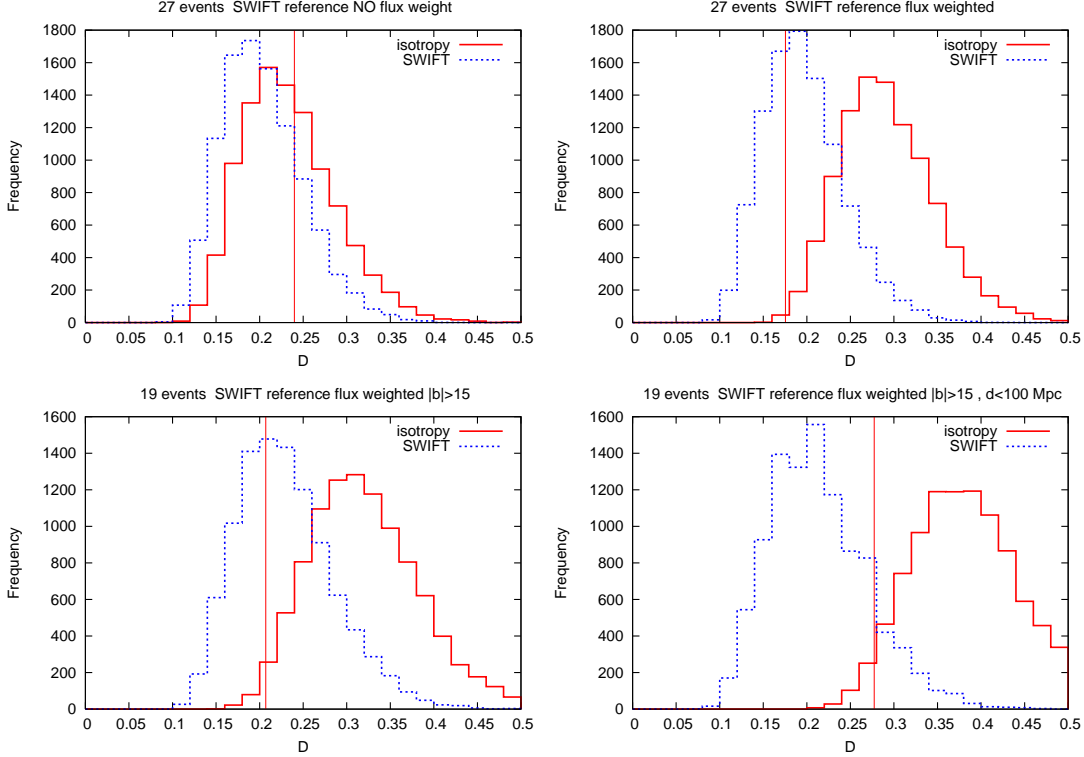


Figure 1: Distribution of 2DKS distances  $D$  between the weighted fractions obtained in different AGN models and the fractions in simulated data samples (according to the same AGN models or to isotropy). The vertical lines correspond to the values obtained for the Auger data.

(corresponding to declinations  $\delta < 24.8^\circ$  for the showers with zenith angle smaller than  $60^\circ$ ). In the top-left panel all these sources are included, weighting them by the relative exposure of the experiment. We always use the equatorial coordinate system to identify the four quadrants with respect to the different reference directions (we have checked that adopting a different coordinate system, such as the galactic one, does not change the qualitative behavior of the results obtained). The two histograms shown correspond to the values obtained for sets of 27 events simulated according to an isotropic distribution or to one generated following the catalog. The vertical line is the distance obtained with the 27 Auger events [4]. It is seen that there is an almost complete overlap between the two histograms, what prevents the possibility of discriminating clearly between the two scenarios (SWIFT AGN sources or isotropy) using this method with the small number of events available at present. The top-right panel is similar but with the sources also weighted by their X ray flux (both in the computation of the cumulative fraction of the catalog and also to obtain the data sample simulated according to the AGN model). Although there is still a significant overlap between the two distributions, the data are in better agreement with the expectations from the AGN based model and only 0.3% of the isotropic simulations have a smaller distance than the data (i.e. the anisotropy probability defined previously is 99.7%). The bottom-left panel is similar to the previous one, i.e. the AGN are also weighted by their X ray flux, but the cut  $|b_G| > 15^\circ$  is imposed, as in [5], what leaves only 19 events in the sample of events from the Auger Observatory. This cut in galactic latitude is inspired in the partial incompleteness of the catalog in regions that could be obscured by the Galaxy. There are however several BAT sources within it (out of 240 AGN seen in the whole sky, 49 are in the region with  $|b_G| < 15^\circ$ , which corresponds to a solid angle of one quarter of the whole sky). The qualitative behavior of the results is very similar as in

the previous plot which included the galactic plane, being the anisotropy probability now 98.2%, a value comparable to the correlation found in [5]. The bottom-right panel further restricts the AGN sample to those closer than 100 Mpc, which are about 40% of the total AGN sample, and in this case  $\sim 3.5\%$  of the isotropic simulations have a value of  $D$  smaller than the data. Compared to the simulations based on the nearby flux-weighted AGN the distance found for the data is still typical.

Turning now to the analysis of the HIPASS galaxy catalog studied in [7], we show in fig. 2 the distribution of distances obtained using as reference model the HIPASS objects, weighted by their total HI line flux  $S_{int}$  and subject to different cuts. We not only show the distribution expected for data simulated according to the particular HIPASS model considered in each panel and the isotropic model expectations, but also show for comparison the distributions obtained for simulated data sets following the SWIFT AGN described before (sampling them according to their X ray fluxes, without imposing the galactic latitude cut and restricting them to those within 100 Mpc). The vertical lines are the corresponding distances  $D$  for the 27 highest energy Auger events.

In the top left panel in fig. 2 we have considered extragalactic HI sources in the northern (NHICAT [9]) and southern (HICAT [8]) HIPASS catalogs. In ref. [7] northern sources were cut at  $S_{int} > 15 \text{ Jy km s}^{-1}$  and southern ones at  $S_{int} > 7.4 \text{ Jy km s}^{-1}$  to have the same completeness level, which was 95% in both samples. We think that keeping objects up to different limiting brightnesses introduces however a non-homogeneity in the two samples stronger than what is obtained keeping the same flux cut for the two samples, even if they end up having different completeness levels. Since the 2DKS test just probes the fractional distribution of objects across the sky, it is important to minimize the possible distortions introduced in the selection process and hence we will adopt the flux limit  $S_{int} > 7.4 \text{ Jy km s}^{-1}$  in both the northern and southern subsamples. With this selection one is left with 3014 HI galaxies in the field of view of the Auger Observatory. As is seen from the plot the distances obtained in the three source models have a significant overlap, and the value obtained with the data set falls just in the overlap region. In particular, being consistent with the isotropic values the resulting anisotropy probability is not large, amounting to 44%.

The top-right panel in fig. 2 is similar but restricted to the HICAT southern sample with declinations  $\delta < 2^\circ$  (and with a cut  $S_{int} > 9.4 \text{ Jy km s}^{-1}$  as in ref [7], for which the flux limited catalog is 99% complete, what leaves 1935 galaxies in this region of the sky). We also restricted the isotropic and AGN based simulations to the southern hemisphere in this plot, and considered only the 25 events from the Auger Observatory falling in the same region of the sky. The results are qualitatively similar to those obtained in the previous plot. The bottom-left panel is further restricted to the galaxies with HI mass<sup>1</sup>  $M_{HI} > 1.1 \times 10^{10} M_\odot$  and distances smaller than 100 Mpc, for which ref. [7] found a maximal correlation. From the results depicted it is seen that the data have a distance smaller than what is obtained in 97% of the isotropic simulations, explaining the large anisotropy probability found. On the other hand, events simulated according to the same model (southern radio galaxies with  $M_{HI} > 1.1 \times 10^{10} M_\odot$  and  $S_{int} > 9.4 \text{ Jy km s}^{-1}$ ) have themselves smaller distances (left histogram) than the isotropic simulations and the distance of the data is quite consistent with them. It is also interesting to note that simulated data following the nearby SWIFT AGN have a distribution of distances (central histogram) somewhat intermediate between the HICAT and isotropic ones. For the present number of events and in this particular comparison, the data are still quite compatible with both the HICAT and SWIFT models, and is only marginally compatible with isotropy. The bottom-right panel in fig. 2 is for a reference catalog obtained restricting the HICAT sample to the galaxies with HI mass bigger than  $2 \times 10^{10} M_\odot$ . We see in this case that the anisotropy probability is about 97%, disfavoring the isotropic hypothesis, but however the same HICAT model would typically give much smaller distances than the data (only 0.3% of the HICAT simulations have a larger value of  $D$  than the data). This implies that the data from the Auger Observatory do not look like a typical realization of this particular model,

---

<sup>1</sup>Following [7], we estimate the HI mass content using  $M/M_\odot \sim 2.36 \times 10^5 d_{Mpc}^2 S_{int}$ , with  $S_{int}$  expressed in [Jy km s<sup>-1</sup>].

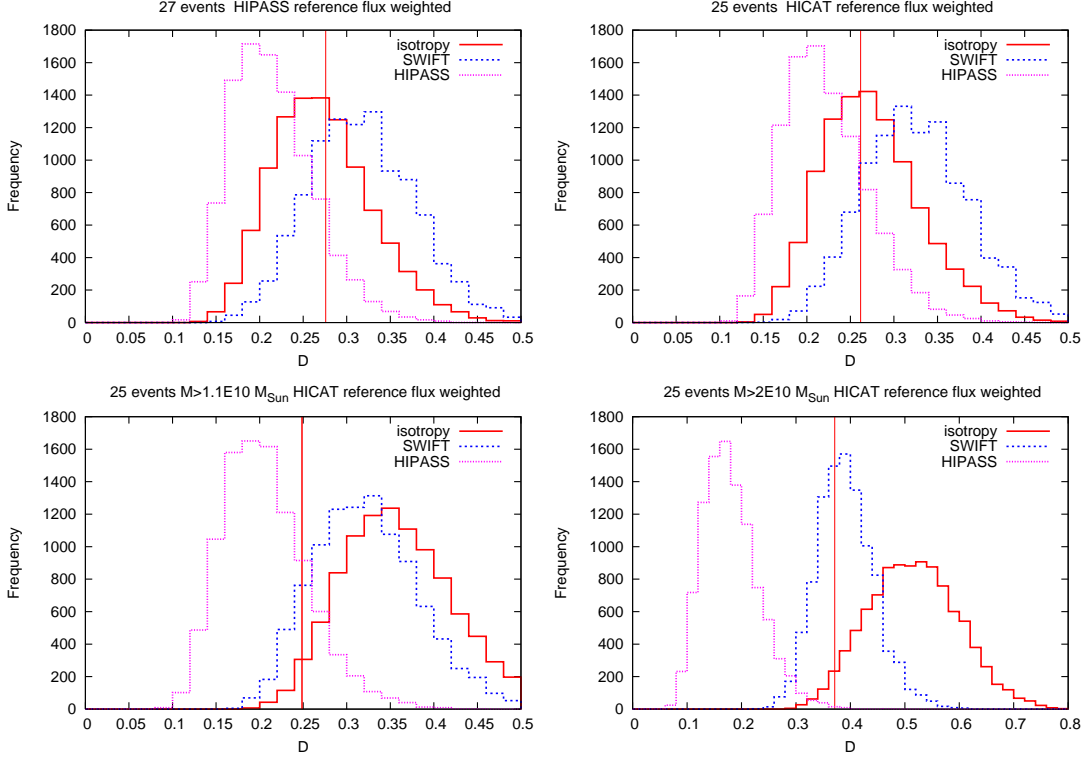


Figure 2: Distribution of 2DKS distances  $D$  between the weighted fractions obtained in different HI galaxy models and the fractions in simulated data samples (according to the same galaxy models (HIPASS), to AGN models (SWIFT) or to isotropy). The vertical lines correspond to the values obtained for the Auger data.

even if the quoted anisotropy probability is large, showing clearly why it is not convenient to call it a correlation probability. On the other hand, in this test the simulations according to the SWIFT AGN model considered give a distribution of distances which encompasses quite comfortably the value found for the data. It is however important to keep in mind that the largest distance between the AGN based models and the reference HIPASS catalog could be in directions (and quadrants) completely different from that giving the largest difference between the data and the HIPASS reference catalog, so that the compatibility found in this particular test does not imply necessarily that the AGN model considered is a good CR source model. In this sense it is important to simultaneously check which is the value of the distance between the data and the SWIFT AGN reference catalog to better establish the compatibility of the data with this particular source model.

From the different plots in fig. 2 one hence concludes that the HIPASS based models considered in the first three panels are all consistent with the data results, while the one in the fourth panel is not. It is also worth noting that the higher level of rejection of isotropy obtained in the third panel doesn't imply necessarily a preference towards sources with  $M_{HI} > 1.1 \times 10^{10} M_{\odot}$ .

Let us also note that in the examples in fig. 2 the data fractions are compared always to the corresponding fractions in the reference catalog used (the flux weighted HIPASS galaxies with different cuts in each panel), and the same is done for the different source models tested (isotropy, SWIFT AGN and HIPASS ones). In fig. 1, which considered the BAT AGN as reference catalog, we didn't show the corresponding histograms for the HIPASS based models just to facilitate the presentation, but the same could have clearly been done. These cross comparisons are quite useful to discriminate among possible source models, and we note that the same can be repeated with other reference catalogs and source scenarios.

## 4 Additional ingredients for the source models

### 4.1 The GZK weight

A possible additional improvement of the source models would be to weight the different sources also by a factor accounting for the suppression of the fluxes above the energy threshold considered due to the GZK effect. One can then account for the expected suppression at the actual distance of each object instead of just eliminating the sources beyond a given specified distance (such as in the examples where only sources within 100 Mpc are kept). This was indeed considered in the past in alternative analyses of the CR arrival direction distributions [14, 15]. The required weight factor  $W_{GZK}$  is the fraction of the events produced above a given threshold  $E_{th}$  which are able to reach a distance equal to the distance from the source to us,  $d$ , with an energy still above that same threshold. Assuming a power law spectrum at the sources  $dN/dE \propto E^{-s}$  this factor is just

$$W_{GZK} = \frac{s-1}{E_{th}^{-s+1}} \int_{E_i(E_{th},d)}^{\infty} dE E^{-s}, \quad (1)$$

where  $E_i(E_{th}, d)$  is the initial energy that a CR must have in order to survive with  $E = E_{th}$  after traveling a distance  $d$ . The resulting factors for  $E_{th} = 60$  and 80 EeV (keep in mind that there are still significant systematic uncertainties in the energy reconstructed in CR experiments) are shown in fig. 3, computed following reference [16]. We assumed a source spectral index of 2.2, but the results are not much sensitive to the particular value adopted, and considered a proton composition. The suppressions are qualitatively similar for Fe nuclei but are stronger for intermediate mass nuclei. Including these factors in the previous comparisons changes the results with respect to those obtained using the simple cutoff at 100 Mpc, but not in a drastic way, although with larger number of events the proper inclusion of the GZK factors could become more important.

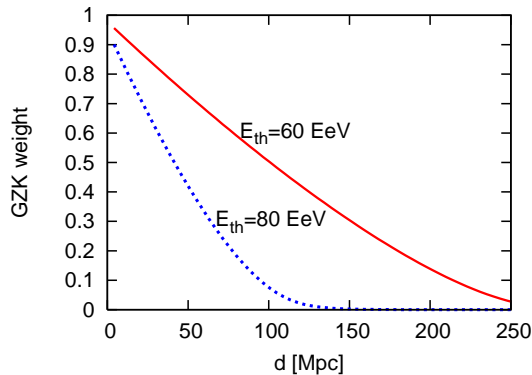


Figure 3: GZK weight vs. distance to the source  $d$  for threshold energies  $E_{th} = 60$  and 80 EeV.

### 4.2 The faint sources

Another aspect that may affect the source models is the fact that the catalogs considered here only contain sources brighter than a certain limit, and although they may be quite complete above those limiting brightnesses, the fraction of sources which are faint increases significantly with increasing distance, and those unobserved sources may actually contribute to the CR fluxes, possibly giving a more diffuse background. In models where the sources are weighted by their fluxes the expected contribution from the unobserved sources is however reduced. In the past some works [14, 15] using the IRAS galaxy catalog, for which the selection effects as a function of distance are

known, corrected for the incompleteness of the catalog by dividing the observed density of galaxies at a given distance by the corresponding selection function in order to obtain a more complete representation of the galaxy distribution. A possible drawback of this approach is that one assigns the unobserved galaxies to the same locations where bright galaxies are observed, and this may not be very precise when the galaxies are sparsely sampled, as happens at large distances. For smaller catalogs, such as the SWIFT one, even if a selection function were known it would not be very realistic to assume that the unobserved faint AGN are in the same locations as the bright ones. Anyway, if one restricts the sources to the nearby ones (using a distance cutoff or weighting them by the GZK attenuation factors), in the models where the sources are weighted by their fluxes the contribution from the faint unobserved sources is not large, so that the model expectations obtained should still be reasonably accurate. For instance, if one models the luminosity distribution of the sources according to a Schechter function<sup>2</sup>,  $dN/dL \propto L^a \exp(-L/L_*)$ , where a typical value for the faint end slope is  $a \simeq -1$ , one finds that the fraction  $F(z)$  of the flux observed above a given flux limit  $f_{min}$  from the sources at redshift  $z$  is  $F(z) \simeq \exp(-f_{min}/f_*)$ , where  $f_*$  is the flux received from an  $L_*$  galaxy lying at redshift  $z$ . In the scenarios in which one assumes that the cosmic ray luminosities are proportional to the observed catalog luminosities (flux weighted scenarios) the fraction  $\eta$  of the total cosmic ray flux which is accounted by the model will then be

$$\eta = \frac{\int dz F(z) W_{GZK}(z)}{\int dz W_{GZK}(z)}. \quad (2)$$

Defining the characteristic depth of the survey  $z_*$  as that corresponding to the redshift at which  $f_* = f_{min}$ , one finds for instance that for the representative value  $z_* = 0.3$  (i.e. about 130 Mpc), the fraction  $\eta$  turns out to be 88% if one uses the GZK attenuation factor corresponding to  $E_{th} = 80$  EeV, while it is 66% if one adopts  $E_{th} = 60$  EeV. For  $z_* = 0.05$  (corresponding to a survey depth of about 200 Mpc), the corresponding fractions are 95% and 82% respectively. Moreover, these fractions become larger in models in which the cosmic ray sources are restricted to those with absolute luminosities above a certain threshold, as was the case for the HIPASS based models restricted to galaxies more massive than a certain limiting mass.

## 5 Prospects with increased statistics

Let us now illustrate the possible discrimination power of the 2DKS test with future increased data samples. For definiteness we use in these examples the GZK factor corresponding to  $E_{th} = 80$  EeV, for which sources beyond 100 Mpc have essentially a negligible contribution and closer ones are weighted non-trivially, and weight the SWIFT and HIPASS sources by their respective fluxes. We consider the HIPASS galaxies (both the northern and southern ones) with  $S_{int} > 7.4$  Jy km s<sup>-1</sup> and  $M_{HI} > 10^{10} M_\odot$ . The left panels in fig. 4 show the distribution of  $D$  values expected for  $n = 50$  and 100 events using as reference catalog the SWIFT one, and the right panels show the results using the HIPASS reference catalog. As a general trend, one can see that the  $D$  distribution of the data sampled according to the reference catalog considered just scales as  $n^{-1/2}$ , peaking at about  $D_{peak} \simeq 0.2\sqrt{25/n}$ , being quite independent from the particular catalog adopted (see also figs. 1 and 2). On the other hand, for the scenarios differing from the reference one (either one based on a different catalog or the isotropic hypothesis), the distribution of  $D$  values tends to a given non-zero average value, with the associated dispersion decreasing as  $n^{-1/2}$ , as is also seen in fig. 4.

It is clear that for 100 events the distributions of the different models become quite separated from each other, and hence this method will have the ability to confidently tell apart these scenarios after a few years of operation of the Auger Observatory. However, as was apparent from figs. 1 and 2, according to the Kolmogorov-Smirnov test the Auger Observatory data analyzed are still

<sup>2</sup>This discussion can be easily extended to the case of a broken power law luminosity function, as that used to fit SWIFT data [6].



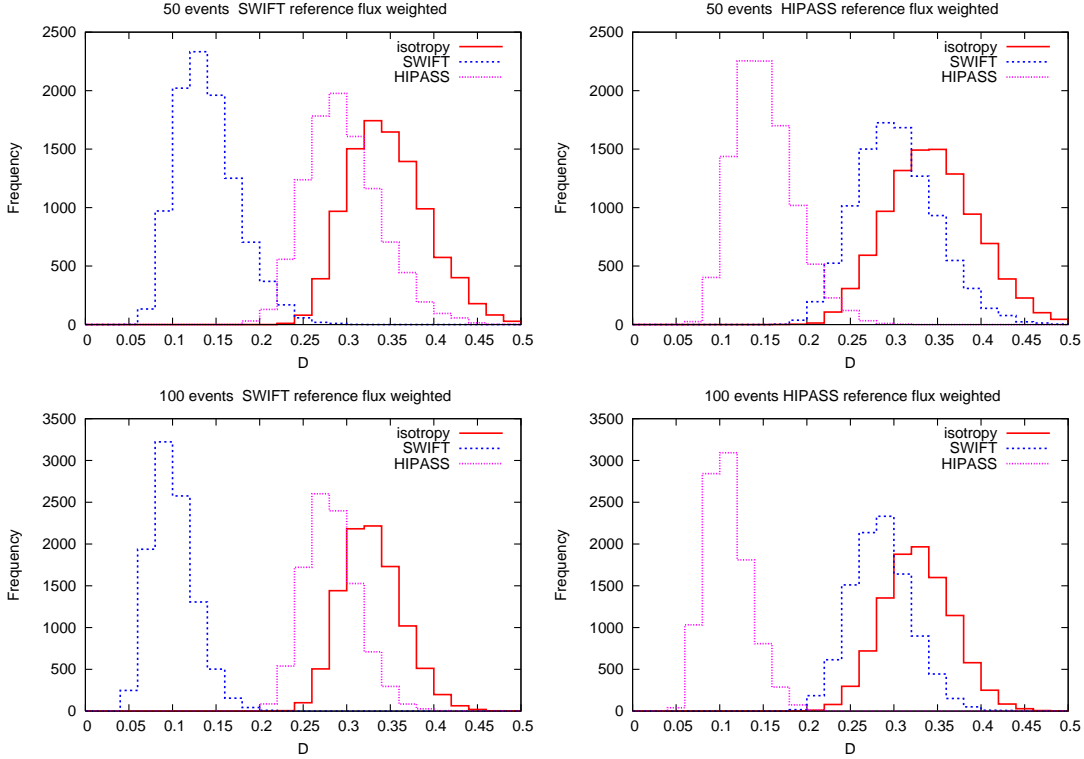


Figure 4: Distribution of 2DKS distances  $D$  between the weighted fractions obtained in models based on AGN from SWIFT, galaxies from HIPASS and isotropy, using as reference catalog the AGN one (left) or HIPASS one (right), for data samples of 50 events (top) or 100 events (bottom).

consistent with many different possible scenarios (except isotropy to a certain level). One has to keep in mind however that the energy threshold for this dataset was selected by the Auger Collaboration as that maximizing the correlation with AGN from the VC catalog, and hence although the discrepancy with isotropy in some of the tests is reassuring, it does not provide a totally independent test of anisotropy.

Finally, it is also useful to consider how would the different sky distributions look for a large number of simulated events, in which case the effects of sampling fluctuations tend to vanish. Identifying the quadrant responsible for the largest fractional difference  $D$  will hence characterize the most important feature discriminating among alternative scenarios in these tests. In particular, when comparing the isotropic and AGN based distributions we find that the largest value of  $D$  arises, in the large data size limit, most frequently from the fourth quadrant, measured in a counter clockwise order starting from the top-right one, with respect to the direction  $(146^\circ, -14^\circ)$ , for which 66% of the weighted AGN lie while only 36% of the isotropic events are found. On the other hand for the HIPASS (north and south with  $S_{int} > 7.4 \text{ Jy km s}^{-1}$ ) flux weighted catalog and the isotropic simulations one finds that the biggest difference is obtained in the first quadrant with respect to the approximate direction  $(225^\circ, -55^\circ)$ , for which the HIPASS simulations have a fraction of about 14% while the isotropic ones of 30%. Also in the fourth quadrant with respect to the direction  $(140^\circ, -30^\circ)$  there is a similar difference, with the HIPASS simulations having a fraction of about 45% while the isotropic ones of 30%. It is mainly these characteristics that may hence allow to differentiate among the possible source populations using this method once a larger number of events become available.

## 6 Discussion

We have considered in some detail the application of the 2DKS test to the study of the distribution of the arrival directions of the UHECRs, extending recent studies of this kind and discussing possible generalizations of the method, in particular introducing the cross comparisons between the distributions of the distances obtained in the different scenarios (not just the isotropic one) and the value of  $D$  obtained with the data. It is important to keep in mind that what the 2DKS test probes is whether the overall distribution of the data is approximately proportional to that of the model considered. This makes the method quite sensitive to the cuts and weights adopted since if only a subsample of the objects in the catalog are the actual sources their distribution in the sky may be quite different from the overall one. In addition, if the assumption that the actual UHECR source luminosities are proportional to the luminosities measured in some particular wavelength (as was the case in most of the models considered) does not hold, the overall CR distribution can be quite different from the one resulting from the model, even if the sources involved are indeed the true CR sources. This may be the strongest limitation of the 2DKS method, and may be a particularly delicate issue if the number of sources contributing to the UHECR events above the threshold energy considered is not large. In this sense the test of correlations performed by the Auger Collaboration is of a different nature, because it just looked for the existence of some AGN within a certain distance and at less than a given angle from the events, without requiring an overall distribution in the sky proportional to the number of objects in the catalog (eventually weighted in some specific way).

As we have shown here, with the enlarged data samples expected in the next few years with the continuous operation of the Auger Observatory it will become possible to test in a significant way several possible models for the distribution of the UHECRs. If the actual CR distribution is different from the model assumptions, this can be put in evidence by comparing the distribution of the simulations according to the particular model and the actual data. The distribution of distances for a model, when one uses the same model as reference, peaks at  $D_{peak} \simeq 1/\sqrt{n}$ , while on the other hand models different from the reference one tend to give rise to larger average distances. Regarding the isotropic simulations, the more anisotropic is the reference catalog to which they are compared, the larger will be the distances obtained, as is apparent from figs. 1 and 2. The 2DKS method can certainly be used as a way to disprove isotropy, and the most efficient way to achieve this will be when using as reference scenario the one closest to the actual source distribution.

## Acknowledgments

We are grateful to Jack Tueller for providing us the 22 months BAT catalog prior to publication and to I. Wong for sending us the NHICAT catalog. This work is supported by ANPCyT (grant PICT 13562-03) and CONICET (grant PIP 5231). We want to thank Paul Sommers for discussions.

## References

- [1] K. Greisen, Phys. Rev. Lett. **16** (1966) 748; G. T. Zatsepin and V. A. Kuzmin, JETP Lett. **4** (1966) 78
- [2] R. U. Abbasi et al. (HiRes Collaboration) Phys. Rev. Lett. **100** (2008) 101101
- [3] The Pierre Auger Collaboration, Phys. Rev. Lett. **101** (2008) 061101
- [4] The Pierre Auger Collaboration *Science* **318** (2007) 939-943; The Pierre Auger Collaboration *Astropart. Phys.* **29** (2008) 188-204
- [5] M. R. George et al., MNRAS **388** (2008) L59

- [6] J. Tueller et al., *Astrophys. J.* **681** (2008) 113
- [7] G. Ghisellini et al., *MNRAS* in press, arXiv:0806.2393 [astro-ph]
- [8] M. J. Meyer et al., *MNRAS* **350** (2004) 1195
- [9] O. I. Wong et al., *MNRAS* **371** (2006) 1855
- [10] J. A. Peacock, *MNRAS* **202** (1983) 615
- [11] G. Fasano and A. Franceschini, *MNRAS* **225** (1987) 155
- [12] S. Singh, C.P. Ma and K. Arons, *Phys. Rev.* **D69** (2004) 063003
- [13] SWIFT BAT 22 months AGN catalog, Jack Tueller private communication
- [14] E. Waxman, K. B. Fisher and T. Piran, *Astrophys. J.* **483** (1997) 1; T. Kashti and E. Waxman, *JCAP* 0805:006 (2008)
- [15] A. Cuoco et al., *JCAP* 01 (2006) 009
- [16] D. Harari, S. Mollerach and E. Roulet, *JCAP* 0611:012 (2006)